

VECTOR WAVE FUNCTIONS IN GYROMAGNETIC UNIAXIAL CHIRAL MEDIUM AND APPLICATIONS

D. Cheng and Y. Antar

Department of Electrical and Computer Engineering
Royal Military College of Canada
Kingston, Ontario, Canada K7K 5L0

- 1. Introduction**
 - 2. Cylindrical Vector Wave Functions**
 - 3. Applications and Convergence Properties of the Cylindrical Vector Wave Functions**
 - 3.1 An Infinitely Long Cylinder with Arbitrary Cross Section
 - 3.2 A Conducting Circular Cylinder with an Inhomogeneous Coating Thickness
 - 3.3 Two Circular Cylinders
 - 4. Concluding Remarks**
- Appendices**
References

1. INTRODUCTION

The vector wave functions, which are first proposed by Hansen to study the electromagnetic radiation problems [1], are important concepts in electromagnetism. This concept, which has been extensively developed by Morse and Feshbach [2], Tai [3], and Zhou [4] in studying the electromagnetic boundary-value problems, seems to gain increasing interest and importance. The vector wave functions have found versatile applications and presented great advantages when compared with other methods (e.g., three-dimensional moment method [5], coupled-dipole method [6], and integral-equation technique [7]). However, the vector wave functions in any given complex media need to be developed, in order to provide methodological convenience in studying the elec-

tromagnetic properties of these materials. Moreover, to establish the reliability and applicability of the vector wave functions in studying the physical properties of the complex media, convergence properties of the series involved must be extensively examined.

Basically, there are five analytical and numerical methods, which are based on the eigenfunction solution of the wave equation, to investigate the electromagnetic phenomena, i.e., the mode-matching method [8], the perturbation approach [9], the T-matrix method [10], the point-matching method [11], and the multipole technique [12]. Despite of the fact that the mode-matching method can provide rigorous criteria for other numerical methods, it is only applicable to simple boundary-value problems which allow the Helmholtz equation to have a separation of variable-based solution. The perturbation method, which involves a Taylor expansion of the fields on the boundary, requires the smallness of the boundary perturbation so that the higher order terms can be neglected. Although the T-matrix method have been widely employed to study the electromagnetic boundary-value problems of isotropic media, this formulation, derived from the Huygens's principle and extinction theorem, requires that the Green dyadic in the exterior region must be expressible in terms of the eigenfunctions. Furthermore, due to the limited knowledge about the Huygens's principle and extinction theorem in complex material, it is often very difficult to obtain the T-matrix formulation. These constraints on the T-matrix method make it unsuitable to investigate the boundary-value problems of complex materials where we can not obtain the eigenfunction expansion of Green dyadic. (For complex materials, the solution of the source-incorporated problems, which involves the Green dyadic, is much more difficult than the source-free one.) Although the point-matching method is not limited by the same constraint condition as T-matrix method, it is well-known that it is more time-consuming for not-the-near-circular or -spherical geometry problems. The multipole technique, which requires the knowledge of the eigenfunction expansion of the field distribution of unit source, is difficult to explore for investigating the physical phenomena of complex materials. Considering the applicability scope of these methods, other computational approaches based on the vector wave functions, which should be superior to these already existing methods, still need to be studied so as to provide the methodological convenience in investigating and exploring the physical phenomena involved in complex materials.

With recent advances in polymer synthesis techniques, increasing attention is being paid to the analysis of interaction of electromagnetic waves with composite materials, in order to determine how to use these materials to provide better solutions to current engineering problems [13–15]. In the present study, a concept of gyromagnetic uniaxial chiral medium is proposed to generalize the well-studied reciprocal chiral medium, gyromagnetic medium, and uniaxial medium with chirality. In practice, a general form of gyromagnetic uniaxial chiral medium can be created by mixing three sets of small metal helices in a host gyromagnetic medium (e.g., magnetically biased ferrite), with the axes of two sets perpendicular and parallel to a fixed direction, respectively, and the other set distributed in random orientations and locations. From a phenomenological point of view, a gyromagnetic uniaxial chiral medium with the preferred axis of z direction can be characterized by a set of constitutive relations

$$\overline{D} = \overline{\overline{\epsilon}} \cdot \overline{E} - \overline{\overline{\xi}} \cdot \overline{H} \quad (1a)$$

$$\overline{B} = \overline{\overline{\mu}} \cdot \overline{H} + \overline{\overline{\xi}} \cdot \overline{E} \quad (1b)$$

where $\overline{\overline{\epsilon}} = \epsilon_t \overline{\overline{I}}_t + \epsilon_z \overline{e}_z \overline{e}_z$, and $\overline{\overline{\mu}} = \mu_t \overline{\overline{I}}_t + \mu_z \overline{e}_z \overline{e}_z - ig \overline{e}_z \times \overline{\overline{I}}_t$ are the permittivity and permeability dyadics, respectively. $\overline{\overline{\xi}} = i(\mu_0 \epsilon_0)^{1/2} (\alpha \overline{\overline{I}}_t + \gamma \overline{e}_z \overline{e}_z)$ is the uniaxial magnetoelectric pseudo-dyadic, where $\overline{\overline{I}}_t = \overline{\overline{I}} - \overline{e}_z \overline{e}_z$ is the transverse unit dyadic, μ_0 and ϵ_0 are the permittivity and permeability of free space, respectively. Here, $\overline{\overline{I}}$ is the unit idem factor and \overline{e}_j represents unit vector in the j direction. α and γ are transverse and axial chirality parameters, respectively. Instead of three parameters for the reciprocal chiral medium, we are facing a medium with seven constitutive parameters, which could provide more flexibility for fabrication design.

To have an idea of a medium with parameter dyadics of the above forms, we first note that the special case with $g = \gamma = 0$ corresponds to the transversely chiral uniaxial bianisotropic medium studied earlier [16]. This medium can be created by scattering metal helices in a dielectric host material in such a way that the axes of all helices are arranged to be perpendicular to the z axis, but possess arbitrary orientations and locations. When $g = \alpha = 0$, this medium is termed as uniaxial chiral medium [17], and can be realized by mixing conductive helices in a dielectric basement medium in such a manner that the axes of all helices are arranged to be parallel to the z axis but

with random locations. For the special case of $\alpha = \gamma$, the material is the already-known chiroferrite medium [18], which can be created by arbitrarily immersing short helices in a magnetized ferrite.

The gyromagnetic uniaxial chiral medium is a subset of the wider class referred to as bianisotropic media. Excellent works in general bianisotropic media have been done by Post [19], Kong [8], and Chen [20] among others. Different from these general considerations, the present investigation is intended to develop the cylindrical vector wave functions to represent the electromagnetic fields in source-free gyromagnetic uniaxial chiral medium and propose an extended mode-matching method to study the two-dimensional electromagnetic boundary-value problems of gyromagnetic uniaxial chiral medium. The formulations of the cylindrical vector wave functions are considerably facilitated by using the concept of characteristic wave and the method of angular spectrum expansion [21]. This extended method leads to compact and explicit expressions of the field representations in terms of the cylindrical vector wave functions. Furthermore, to make the efficient recursive algorithm developed by Chew [22] available to layered structures and multiple scatterers consisting of gyromagnetic uniaxial chiral media, an outline to derive the addition theorem of the vector wave functions for gyromagnetic uniaxial chiral medium is described. For applications of the present cylindrical vector wave functions, an extended mode-matching method is proposed to study the two-dimensional electromagnetic scattering of a cylinder with arbitrary cross section and a conducting circular cylinder with an inhomogeneous coating thickness. To check the convergence of the present cylindrical vector wave functions for multiple-body problem, electromagnetic scattering by two circular cylinders of gyromagnetic uniaxial chiral media is also investigated. Excellent convergence properties of the cylindrical vector wave functions in these application examples are numerically verified, which establishes the reliability and applicability of the present formulation.

This manuscript is organized as follows. In Sec. 2, based on the concept of characteristic waves and the method of angular spectral expansion, the cylindrical vector wave functions in source-free gyromagnetic uniaxial chiral medium are developed to represent the electromagnetic field. It is found that the solutions of the source-free vector wave equation for gyromagnetic uniaxial chiral medium are composed of two transverse waves and a longitudinal wave. Addition theorem

of the vector wave functions for gyromagnetic uniaxial chiral medium can be directly obtained from its counterpart for isotropic medium. In Sec. 3, to illustrate how to use the present cylindrical vector wave functions in a practical way and examine the convergence properties of the infinite series involved, an extended mode-matching method is proposed to study the electromagnetic scattering of a gyromagnetic uniaxial chiral cylinder with arbitrary cross section and a conducting circular cylinder with an inhomogeneous coating thickness of gyromagnetic uniaxial chiral medium. To check the convergence of the present cylindrical vector wave functions for multiple-body problem, electromagnetic scattering by two circular cylinders of gyromagnetic uniaxial chiral media is also investigated. The formulations for these numerical calculation are briefly described in this context, and for the sake of consistency the details are arranged in the Appendices. Extensive computations reveal that the infinite series involved in these application examples have the excellent convergence properties, which establishes the reliability and applicability of the present cylindrical vector wave functions. Sec. 4 concludes this manuscript with a remark on the present cylindrical vector wave functions and the extended mode-matching method.

In the following analysis, the harmonic $\exp(i\omega t)$ time dependence is assumed and suppressed. In the notations we adopted, double overline is used to represent dyadics and overline is used for vectors.

2. CYLINDRICAL VECTOR WAVE FUNCTIONS

In this section, we will try to give the eigenfunction expansion of the electromagnetic waves in a gyromagnetic uniaxial chiral medium, based on the concept of characteristic waves and the method of angular spectral expansion [21].

Substituting the constitutive relations (1a) and (1b) into the source-free Maxwell's equations, a $\overline{\overline{H}}$ -field vector wave equation is obtained

$$\nabla \times \overline{\overline{\epsilon}}^{-1} \cdot \nabla \times \overline{\overline{H}} + i\omega (\nabla \times \overline{\overline{\epsilon}}^{-1} \cdot \overline{\overline{\xi}} \cdot \overline{\overline{H}} + \overline{\overline{\xi}} \cdot \overline{\overline{\epsilon}}^{-1} \cdot \nabla \times \overline{\overline{H}}) - \omega^2 (\overline{\overline{\mu}} + \overline{\overline{\xi}} \cdot \overline{\overline{\epsilon}}^{-1} \cdot \overline{\overline{\xi}}) \cdot \overline{\overline{H}} = 0 \quad (2)$$

The characteristic waves corresponding to (2) can be examined in the Fourier transform domain, which leads to the characteristic equation

$$a\epsilon' k_\rho^4 - [(k_z^2 - a)(a + a'\epsilon' - e^2) - (bk_z + c)(bk_z - 2ek_z + c)]k_\rho^2 + [(k_z^2 - a)^2 + (bk_z + c)^2]a' = 0 \quad (3)$$

where

$$\begin{aligned} a &= \omega^2(\varepsilon_t \mu_t - \varepsilon_0 \mu_0 \alpha^2) \\ b &= 2ik_0 \alpha \\ c &= i\omega^2 \varepsilon_t g \\ e &= ik_0(\alpha + \varepsilon' \gamma) \\ a' &= \omega^2(\varepsilon_t \mu_z - \varepsilon_0 \mu_0 \gamma^2 \varepsilon') \end{aligned}$$

and $k_0 = \omega(\varepsilon_0 \mu_0)^{1/2}$, $\varepsilon' = \varepsilon_t / \varepsilon_z$.

Designating the roots of (3) as $k_\rho = k_{\rho q}$ ($q = 1, 2, 3, 4$), the magnetic eigenwaves can be written as

$$\begin{aligned} \overline{H}_q(k_z, \phi_k) &= [A_q(k_z) \cos(\phi - \phi_k) + B_q(k_z) \sin(\phi - \phi_k)] \overline{e}_\rho \\ &\quad + [-A_q(k_z) \sin(\phi - \phi_k) + B_q(k_z) \cos(\phi - \phi_k)] \overline{e}_\phi + \overline{e}_z \end{aligned} \quad (4)$$

where

$$A_q(k_z) = k_{\rho q} \frac{k_z(\varepsilon' k_{\rho q}^2 + k_z^2 - a) + e(bk_z + c)}{D_q(k_z)} \quad (5a)$$

$$B_q(k_z) = k_{\rho q} \frac{e(k_z^2 - a) - (bk_z + c)k_z}{D_q(k_z)} \quad (5b)$$

$$D_q(k_z) = (k_z^2 - a)(\varepsilon' k_{\rho q}^2 + k_z^2 - a) + (bk_z + c)^2 \quad (5c)$$

The magnetic field is then written as

$$\begin{aligned} \overline{H}(\vec{r}) &= \sum_{q=1}^2 \int_{-\infty}^{\infty} dk_z \int_{\phi_k=0}^{2\pi} d\phi_k e^{-i[k_z z + k_{\rho q} \rho \cos(\phi - \phi_k)]} \\ &\quad \overline{H}_q(k_z, \phi_k) H_{qz}(k_z, \phi_k) \end{aligned} \quad (6a)$$

where $H_{qz}(k_z, \phi_k)$ is the amplitude of the spectral longitudinal component of magnetic field. Applying the angular spectral expansion [21] to $H_{qz}(k_z, \phi_k)$

$$H_{qz}(k_z, \phi_k) = \sum_{n=-\infty}^{\infty} h_{qn}(k_z) e^{-in\phi_k} \quad (6b)$$

and after some mathematical manipulation, we obtain (see Appendix

A for detail)

$$\begin{aligned} \overline{H}(\vec{r}) = & \pi \sum_{q=1}^2 \int_{-\infty}^{\infty} dk_z \sum_{n=-\infty}^{\infty} (-i)^n h_{qn}(k_z) [A_q^h(k_z) \overline{M}_n^{(1)}(k_z, k_{\rho q}) \\ & + B_q^h(k_z) \overline{N}_n^{(1)}(k_z, k_{\rho q}) + C_q^h(k_z) \overline{L}_n^{(1)}(k_z, k_{\rho q})] \end{aligned} \quad (7)$$

where the cylindrical vector wave functions are defined as

$$\overline{M}_n^{(j)}(k_z, k_{\rho q}) = \nabla \times [\Psi_n^{(j)}(k_z, k_{\rho q}) \vec{e}_z] \quad (8a)$$

$$\overline{N}_n^{(j)}(k_z, k_{\rho q}) = \frac{1}{k_q} \nabla \times \overline{M}_n^{(j)}(k_z, k_{\rho q}) \quad (8b)$$

$$\overline{L}_n^{(j)}(k_z, k_{\rho q}) = \nabla [\Psi_n^{(j)}(k_z, k_{\rho q})] \quad (8c)$$

with

$$\Psi_n^{(j)}(k_z, k_{\rho q}) = Z_n^{(j)}(k_{\rho q} \rho) \exp[-i(k_z z + n\phi)]$$

and

$$k_q = (k_{\rho q}^2 + k_z^2)^{1/2}.$$

Here, $Z_n^{(j)} = J_n(\cdot)$, $Y_n(\cdot)$, $H_n^{(1)}(\cdot)$, and $H_n^{(2)}(\cdot)$, for $j = 1, 2, 3$, and 4, respectively. The expansion coefficients of the vector wave functions are found to be

$$A_q^h(k_z) = -\frac{2iB_q(k_z)}{k_{\rho q}} \quad (9a)$$

$$B_q^h(k_z) = -\frac{2k_q A_q(k_z)}{(k_{\rho q} k_z)} + \frac{2[1 + k_{\rho q} A_q(k_z)/k_z]}{k_q} \quad (9b)$$

$$C_q^h(k_z) = \frac{2ik_z[1 + k_{\rho q} A_q(k_z)/k_z]}{k_q^2} \quad (9c)$$

The electric field can be easily obtained from the Maxell's equations, and straightforward algebraic manipulation leads to

$$\begin{aligned} \overline{E}(\vec{r}) = & \pi \sum_{q=1}^2 \int_{-\infty}^{\infty} dk_z \sum_{n=-\infty}^{\infty} (-i)^n h_{qn}(k_z) [A_q^e(k_z) \overline{M}_n^{(1)}(k_z, k_{\rho q}) \\ & + B_q^e(k_z) \overline{N}_n^{(1)}(k_z, k_{\rho q}) + C_q^e(k_z) \overline{L}_n^{(1)}(k_z, k_{\rho q})] \end{aligned} \quad (10)$$

where the weighted coefficients of the vector wave functions are determined as

$$A_q^e(k_z) = \frac{ik_q B_q^h(k_z)}{\omega \varepsilon_t} + \frac{ik_0 \alpha A_q^h(k_z)}{\omega \varepsilon_t} \quad (11a)$$

$$B_q^e(k_z) = -\frac{iA_q^h(k_z)}{\omega k_q} \left(\frac{k_z^2}{\varepsilon_t} + \frac{k_{\rho q}^2}{\varepsilon_z} \right) + \frac{ik_0 B_q^h(k_z)}{\omega k_q^2} \left(\frac{k_z^2 \alpha}{\varepsilon_t} - \frac{k_{\rho q}^2 \gamma}{\varepsilon_z} \right) - \frac{k_0 k_z C_q^h(k_z)}{\omega k_q} \left(\frac{\alpha}{\varepsilon_t} - \frac{\gamma}{\varepsilon_z} \right) \quad (11b)$$

$$C_q^e(k_z) = -\frac{k_z A_q^h(k_z)}{\omega \varepsilon_t} + \frac{ik_z B_q^e(k_z)}{k_q} + \frac{ik_0 \alpha}{\omega \varepsilon_t} \left[C_q^h(k_z) - \frac{ik_z}{k_q} B_q^h(k_z) \right] \quad (11c)$$

Since Bessel, Neuman, and Hankel functions of the same order satisfy the identical differential equation, the first kind of vector wave functions in equations (7) and (10) can be generalized to the three other sets, corresponding to Neuman and Hankel functions.

The resulting equations (7) and (10) indicate that solutions of the source-free Maxwell equations in gyromagnetic uniaxial chiral medium, which can be represented in terms of the cylindrical vector wave functions, are superposition of two transverse waves (TE for \overline{M} and TM for \overline{N}) and a longitudinal wave.

To make the efficient recursive algorithm developed by Chew [22] available to layered structures and multiple scatterers consisting of gyromagnetic uniaxial chiral media, the addition theorem of the cylindrical vector wave functions for gyromagnetic uniaxial chiral medium can be directly obtained by substituting the counterpart for isotropic medium [22] in (7) and (10).

3. APPLICATIONS AND CONVERGENCE PROPERTIES OF THE CYLINDRICAL VECTOR WAVE FUNCTIONS

To illustrate how to use the present cylindrical vector wave functions in a practical way and to examine the convergence properties of the infinite series involved, an extended mode-matching method is proposed to study the electromagnetic scattering of a cylinder with arbitrary cross section and a conducting circular cylinder with an inhomogeneous coating thickness. To check the convergence of the present cylindrical

vector wave functions for multiple-body problem, electromagnetic scattering by two circular cylinders of gyromagnetic uniaxial chiral media is also investigated.

3.1 An Infinitely Long cylinder with Arbitrary Cross Section

In this subsection, we will try to develop an extended mode-matching method to study the electromagnetic scattering of a cylinder with arbitrary cross section. For this purpose, we first choose the coordinate system so that the incident wave is along $+x$ axis. The cylinder is bounded by the surface $\rho = f(\phi)$, where $f'(\phi)$ is a single value and continuous function of ϕ .

Since an arbitrary polarized electromagnetic wave in free space can be decomposed into TM_z and TE_z polarized waves which are independent and dual with each other, we will only consider the TM_z incident case without losing any generality. The incident TM_z wave of unit amplitude of electric field is expanded in terms of the circular cylindrical vector wave functions

$$\overline{E}^{inc}(\vec{r}) = \bar{e}_z e^{-ik_0 x} = \int_{-\infty}^{\infty} dk_z \sum_{n=-\infty}^{\infty} (-i)^n \delta(k_z) \overline{N}_n^{(1)}(k_z, k_\rho) / k_0 \quad (12a)$$

$$\begin{aligned} \overline{H}^{inc}(\vec{r}) &= -\frac{i\bar{e}_y e^{-ik_0 x}}{\eta_0} \\ &= \int_{-\infty}^{\infty} dk_z \sum_{n=-\infty}^{\infty} (-i)^{n-1} \delta(k_z) \overline{M}_n^{(1)}(k_z, k_\rho) / (k_0 \eta_0) \end{aligned} \quad (12b)$$

where $k_\rho = (k_0^2 - k_z^2)^{1/2}$, and $\delta(\cdot)$ is the Dirac delta function. Here, $k_0 = \omega(\epsilon_0 \mu_0)^{1/2}$ and $\eta_0 = (\mu_0 / \epsilon_0)^{1/2}$ represent the wave number and wave impedance of free space, respectively. The scattered electromagnetic waves may have TM_z and TE_z components and should be expanded as

$$\overline{E}^{sca}(\vec{r}) = \int_{-\infty}^{\infty} dk_z \sum_{n=-\infty}^{\infty} (-i)^n [a_n \overline{M}_n^{(4)}(k_z, k_\rho) + b_n \overline{N}_n^{(4)}(k_z, k_\rho)] \quad (13a)$$

$$\overline{H}^{sca}(\vec{r}) = \int_{-\infty}^{\infty} dk_z \sum_{n=-\infty}^{\infty} (-i)^{n-1} / \eta_0 [a_n \overline{N}_n^{(4)}(k_z, k_\rho) + b_n \overline{M}_n^{(4)}(k_z, k_\rho)] \quad (13b)$$

In the expressions (12) and (13), the functions $\overline{M}_n^{(j)}(k_z, k_\rho)$ and $\overline{N}_n^{(j)}(k_z, k_\rho)$ ($j = 1, 4$) are the cylindrical vector wave functions as defined in the previous section.

The electromagnetic fields excited inside the scatterer $\overline{E}^{int}(\overline{r})$, $\overline{H}^{int}(\overline{r})$ can be represented in terms of the cylindrical vector wave functions in the way we have presented in the previous section.

The boundary conditions to ensure the continuity of the electric and magnetic fields at the outer surface of the scatterer $\rho = f(\phi)$ are

$$E_\rho^{int} \sin \theta + E_\phi^{int} \cos \theta = (E_\rho^{inc} + E_\rho^{sca}) \sin \theta + (E_\phi^{inc} + E_\phi^{sca}) \cos \theta \quad (14a)$$

$$E_z^{int} = E_z^{inc} + E_z^{sca} \quad (14b)$$

$$H_\rho^{int} \sin \theta + H_\phi^{int} \cos \theta = (H_\rho^{inc} + H_\rho^{sca}) \sin \theta + (H_\phi^{inc} + H_\phi^{sca}) \cos \theta \quad (14c)$$

$$H_z^{int} = H_z^{inc} + H_z^{sca} \quad (14d)$$

where all the field components are evaluated at $\rho = f(\phi)$, and

$$\theta = \tan^{-1} \left(\frac{f'(\phi)}{f(\phi)} \right)$$

To numerically solve Eqs. (14a–14d), the infinite series involved must be truncated. In what follows, the infinite summation is such truncated that the series is taken to be summed up from $-N$ to N . These truncated equations can be easily analytically solved for the expansion coefficients of the scattered fields. For the sake of consistency, details for the formulations of the solution procedure are organized in Appendix B. After carefully examining the final numerical results, excellent convergent properties of these truncated series are established, which make the truncating process reasonable.

The bistatic echo width, which represents the density of the power scattered by the cylindrical object, is defined as

$$A_\sigma(\phi) = \lim_{\rho \rightarrow \infty} 2\pi\rho \frac{\text{Re}\{[\overline{E}^{sca}(\overline{r})] \times [\overline{H}^{sca}(\overline{r})]^*\} \cdot \overline{e}_\rho}{\text{Re}\{[\overline{E}^{inc}(\overline{r})] \times [\overline{H}^{inc}(\overline{r})]^*\} \cdot \overline{e}_x} \quad (15)$$

where the asterisk indicates complex conjugate, and $\text{Re}[\cdot]$ denotes real part of the complex function.

Recalling the asymptotic expression of the Hankel function in the far region

$$H_n^{(2)}(k_0\rho) = \sqrt{\frac{2}{\pi k_0\rho}} e^{-i[k_0\rho - (2n+1)\pi/4]} \quad \rho \rightarrow \infty \quad (16)$$

we can rewrite the expression (15) in a more explicit form

$$A_\sigma(\phi) = 4k_0 \left[\left| \sum_{n=-\infty}^{\infty} a_n e^{-in\phi} \right|^2 + \left| \sum_{n=-\infty}^{\infty} b_n e^{-in\phi} \right|^2 \right] \quad (17)$$

To validate this extended mode-matching process, numerical results of the present method for the scattering by a circular cylinder ($\rho = a$) and a deviated circular cylinder ($\rho = b \cos \phi + \sqrt{b^2 \cos^2 \phi + a^2 - b^2}$, $b < a$) have been computed and compared with that of a circular cylinder calculated by the conventional mode-matching method, respectively. Excellent agreement between the results is obtained. For completeness and comparison purposes, formulations of the conventional mode-matching method for scattering by a circular cylinder are presented in Appendix C.

Previous to the actual computation for the scattering by a gyromagnetic uniaxial chiral cylinder with noncircular cross section, convergence of the results involved must be examined. Table 1 presents the numerical results of the convergence test for a gyromagnetic uniaxial chiral cylinder of elliptical cross section. It is seen that by properly choosing the truncated number N of the series involved, reliable results can be obtained for all scattering angles. The convergence check indicates that the present cylindrical vector wave functions in conjunction with the extended mode-matching method can be reliably applied to study the two-dimensional electromagnetic phenomena of single gyromagnetic uniaxial chiral object. To provide criteria for other numerical method, Figure 1 illustrates the bistatic echo width of an elliptical cylinder of gyromagnetic uniaxial chiral medium.

3.2 A Conducting Circular Cylinder with an Inhomogeneous Coating Thickness

In this subsection, we will try to use the extended mode-matching method to study the electromagnetic scattering of a conducting cylinder with an arbitrary coating thickness of gyromagnetic uniaxial chiral

A_σ/λ_0 (dB)	$\phi = 0^\circ$	$\phi = 45^\circ$	$\phi = 90^\circ$
$N = 3$	0.12248 <i>D</i> + 02	0.10087 <i>D</i> + 01	-0.10200 <i>D</i> + 02
$N = 7$	0.17750 <i>D</i> + 02	0.74789 <i>D</i> + 01	0.42195 <i>D</i> + 01
$N = 9$	0.17641 <i>D</i> + 02	0.83354 <i>D</i> + 01	0.53105 <i>D</i> + 01
$N = 11$	0.17603 <i>D</i> + 02	0.82464 <i>D</i> + 01	0.51759 <i>D</i> + 01
$N = 13$	0.17606 <i>D</i> + 02	0.82476 <i>D</i> + 01	0.51678 <i>D</i> + 01
$N = 15$	0.17606 <i>D</i> + 02	0.82477 <i>D</i> + 01	0.51675 <i>D</i> + 01
$N = 16$	0.17606 <i>D</i> + 02	0.82477 <i>D</i> + 01	0.51675 <i>D</i> + 01
$N = 17$	0.17606 <i>D</i> + 02	0.82477 <i>D</i> + 01	0.51675 <i>D</i> + 01
$N = 18$	0.17606 <i>D</i> + 02	0.82477 <i>D</i> + 01	0.51675 <i>D</i> + 01
$N = 20$	0.17606 <i>D</i> + 02	0.82477 <i>D</i> + 01	0.51675 <i>D</i> + 01
A_σ/λ_0 (dB)	$\phi = 135^\circ$		$\phi = 180^\circ$
$N = 3$	-0.38507 <i>D</i> + 00		0.32435 <i>D</i> + 01
$N = 7$	0.24402 <i>D</i> + 01		0.58899 <i>D</i> + 01
$N = 9$	0.76054 <i>D</i> + 00		0.58976 <i>D</i> + 01
$N = 11$	0.14773 <i>D</i> + 00		0.58830 <i>D</i> + 01
$N = 13$	0.84954 <i>D</i> - 01		0.58773 <i>D</i> + 01
$N = 15$	0.81675 <i>D</i> - 01		0.58773 <i>D</i> + 01
$N = 16$	0.81573 <i>D</i> - 01		0.58773 <i>D</i> + 01
$N = 17$	0.81568 <i>D</i> - 01		0.58773 <i>D</i> + 01
$N = 18$	0.81566 <i>D</i> - 01		0.58773 <i>D</i> + 01
$N = 20$	0.81566 <i>D</i> - 01		0.58773 <i>D</i> + 01

Table 1. Convergence test of an elliptical cylinder of gyromagnetic uniaxial chiral medium (TM_z). The constitutive parameters of the scatterer are taken to be as $\mu_t/\mu_0 = 1.8$, $\mu_z/\mu_0 = 1.2$, $g/\mu_0 = 0.12$, $\varepsilon_t/\varepsilon_0 = 2.5$, $\varepsilon_z/\varepsilon_0 = 2.1$, $\alpha = 0.3$, and $\gamma = 0.7$. The geometry parameters of the scatterer are taken to be semi major axis = $1.2\lambda_0$, and semi minor axis = $0.9\lambda_0$. The major axial of the scatterer takes an angle of $2\pi/9$ with respect to the x axis.

medium. For this purpose, we also fix the coordinate system so that the incident wave is along the $+x$ axis, the conducting core is bounded by $\rho = a$, and the outer surface is bounded by the surface $\rho = f(\phi)$, where $f'(\phi)$ is a single value and continuous function of ϕ .

Once again, the TM_z incident wave with unit amplitude of electric field is considered. The incident and scattered waves are expanded in

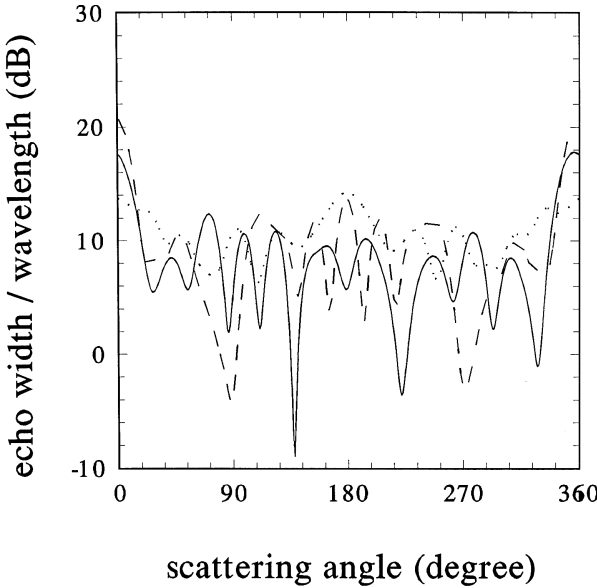


Figure 1. Scattering pattern of an elliptical gyromagnetic uniaxial chiral cylinder due to a normally incident TM_z polarized plane wave. The geometrical and constitutive parameters are taken to be as the same as those of Table 1. The dotted line corresponds to the case where the major axial of the scatterer is along the x axis, the dashed line for the major axis along the y axis, and the solid line for the major axis having an angle of $2\pi/9$ with respect to the x axis.

terms of the cylindrical vector wave functions, as Eqs. (12) and (13). According to the cylindrical wave functions in gyromagnetic uniaxial chiral material developed in Section 2, the fields in the coating region can be represented as

$$\begin{aligned} \overline{E}^{int} = & \sum_{q=1}^2 \sum_{n=-\infty}^{\infty} (-i)^n \left\{ h_{qn}^{(1)} [A_q^e \overline{M}_n^{(1)}(k_{\rho q}) + B_q^e \overline{N}_n^{(1)}(k_{\rho q}) + C_q^e \overline{L}_n^{(1)}(k_{\rho q})] \right. \\ & \left. + h_{qn}^{(4)} [A_q^e \overline{M}_n^{(4)}(k_{\rho q}) + B_q^e \overline{N}_n^{(4)}(k_{\rho q}) + C_q^e \overline{L}_n^{(4)}(k_{\rho q})] \right\} \end{aligned} \quad (18a)$$

$$\begin{aligned} \overline{H}^{int} = & \sum_{q=1}^2 \sum_{n=-\infty}^{\infty} (-i)^n \left\{ h_{qn}^{(1)} [A_q^h \overline{M}_n^{(1)}(k_{\rho q}) + B_q^h \overline{N}_n^{(1)}(k_{\rho q}) + C_q^h \overline{L}_n^{(1)}(k_{\rho q})] \right. \\ & \left. + h_{qn}^{(4)} [A_q^h \overline{M}_n^{(4)}(k_{\rho q}) + B_q^h \overline{N}_n^{(4)}(k_{\rho q}) + C_q^h \overline{L}_n^{(4)}(k_{\rho q})] \right\} \end{aligned} \quad (18b)$$

where $h_{qn}^{(1)}$ and $h_{qn}^{(4)}$ ($q = 1, 2$) are expansion coefficients. Here, $k_z = 0$ for the cylindrical vector wave functions and their weighted coefficients have been suppressed for the sake of writing simplicity.

The boundary conditions at the boundary $\rho = a$ are

$$E_z^{int}|_{\rho=a} = 0 \quad (19a)$$

$$E_\phi^{int}|_{\rho=a} = 0 \quad (19b)$$

And the boundary conditions at outer surface of the scatterer $\rho = f(\phi)$ are

$$E_\rho^{int} \sin \theta + E_\phi^{int} \cos \theta = (E_\rho^{inc} + E_\rho^{sca}) \sin \theta + (E_\phi^{inc} + E_\phi^{sca}) \cos \theta \quad (20a)$$

$$E_z^{int} = E_z^{inc} + E_z^{sca} \quad (20b)$$

$$H_\rho^{int} \sin \theta + H_\phi^{int} \cos \theta = (H_\rho^{inc} + H_\rho^{sca}) \sin \theta + (H_\phi^{inc} + H_\phi^{sca}) \cos \theta \quad (20c)$$

$$H_z^{int} = H_z^{inc} + H_z^{sca} \quad (20d)$$

where all the field components are evaluated at $\rho = f(\phi)$, and

$$\theta = \tan^{-1} \left(\frac{f'(\phi)}{f(\phi)} \right)$$

To numerically solve Eqs. (19) and (20), the infinite series involved must be truncated. These truncated equations can be easily solved for the expansion coefficients of the scattered fields. For the sake of consistency, details for the formulations of the solution procedure are organized in Appendix D.

To validate this extended mode-matching process, numerical results of the present method for the solution of a conducting circular cylinder with a coaxial coating are computed and compared with those calculated by the conventional mode-matching method. Excellent agreement between the results is obtained.

Similar to Subsection 3.1, convergence test of the results involved should be carefully examined for the scattering of a conducting circular cylinder with an inhomogeneous coating thickness of gyromagnetic uniaxial chiral medium. Table 2 presents the numerical results for

A_σ/λ_0 (dB)	$\phi = 0^\circ$	$\phi = 45^\circ$	$\phi = 90^\circ$
$N = 3$	0.99952 <i>D</i> + 01	-0.19771 <i>D</i> + 01	0.28603 <i>D</i> + 01
$N = 7$	0.17444 <i>D</i> + 02	0.13912 <i>D</i> + 01	0.15692 <i>D</i> + 02
$N = 9$	0.18661 <i>D</i> + 02	0.17019 <i>D</i> + 02	0.17470 <i>D</i> + 02
$N = 11$	0.18698 <i>D</i> + 02	0.17418 <i>D</i> + 02	0.16877 <i>D</i> + 02
$N = 13$	0.18646 <i>D</i> + 02	0.17482 <i>D</i> + 02	0.16867 <i>D</i> + 02
$N = 15$	0.18648 <i>D</i> + 02	0.17473 <i>D</i> + 02	0.16856 <i>D</i> + 02
$N = 16$	0.18648 <i>D</i> + 02	0.17473 <i>D</i> + 02	0.16856 <i>D</i> + 02
$N = 17$	0.18648 <i>D</i> + 02	0.17473 <i>D</i> + 02	0.16856 <i>D</i> + 02
$N = 18$	0.18648 <i>D</i> + 02	0.17473 <i>D</i> + 02	0.16856 <i>D</i> + 02
$N = 20$	0.18648 <i>D</i> + 02	0.17473 <i>D</i> + 02	0.16856 <i>D</i> + 02
A_σ/λ_0 (dB)	$\phi = 135^\circ$		$\phi = 180^\circ$
$N = 3$	0.38507 <i>D</i> + 01		0.80001 <i>D</i> + 01
$N = 7$	0.69330 <i>D</i> + 01		0.14340 <i>D</i> + 02
$N = 9$	0.81463 <i>D</i> + 01		0.16822 <i>D</i> + 02
$N = 11$	0.80086 <i>D</i> + 01		0.16061 <i>D</i> + 02
$N = 13$	0.80362 <i>D</i> + 01		0.15947 <i>D</i> + 02
$N = 15$	0.80479 <i>D</i> + 01		0.15938 <i>D</i> + 02
$N = 16$	0.80480 <i>D</i> + 01		0.15938 <i>D</i> + 02
$N = 17$	0.80487 <i>D</i> + 01		0.15939 <i>D</i> + 02
$N = 18$	0.80488 <i>D</i> + 01		0.15939 <i>D</i> + 02
$N = 20$	0.80488 <i>D</i> + 01		0.15939 <i>D</i> + 02

Table 2. Convergence test of a conducting cylinder with a coating of elliptical cross section (TM_z). The constitutive parameters of the coating are taken to be the same as those of Table 1. The elliptical-shaped coating has a semi major axis of $1.4\lambda_0$, and semi minor axis $1.1\lambda_0$, the radius of the conducting cone is $0.8\lambda_0$. The major axial of the cross section of the coating takes an angle of $2\pi/9$ with respect to the x axis.

the convergence test for a conducting circular cylinder with a gyromagnetic uniaxial chiral coating of elliptical cross section. It is seen that for proper truncated number N , reliable results can be obtained for all scattering angles. The convergence check indicates that the present cylindrical vector wave functions in association with the extended mode-matching method can be reliably utilized to investigate

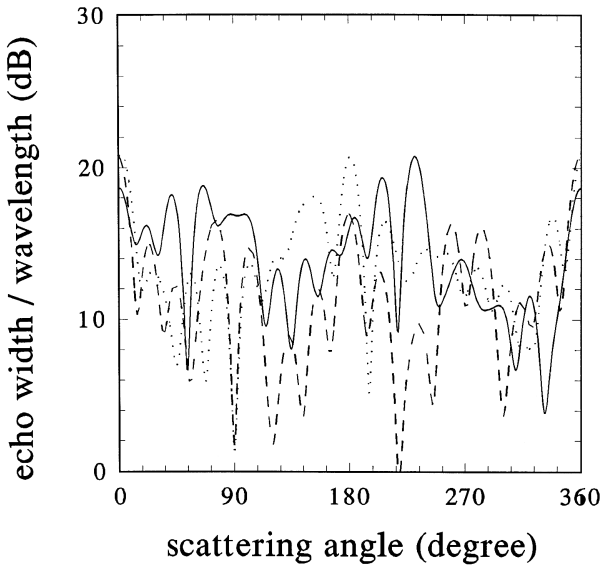


Figure 2. Scattering pattern of a conducting circular cylinder with a coating of elliptical cross section, due to a normally incident TM_z polarized plane wave. The geometrical and constitutive parameters are taken to be the same as those of Table 2. The dotted line corresponds to the case where the major axis of the coating is along the x axis, the dashed line for the major axis along the y axis, and the solid line for the major axis having an angle of $2\pi/9$ with respect to the x axis.

the two-dimensional boundary-value problem of multilayered gyromagnetic uniaxial chiral objects. To provide criteria for other numerical method, Figure 2 illustrates the bistatic echo width of a conducting circular cylinder with a gyromagnetic uniaxial chiral coating of elliptical cross section.

3.3 Two Circular Cylinders

To illustrate the applicability of the present cylindrical vector wave functions for multiple scattering problems, we now try to use the addition theorem to study the electromagnetic scattering of two circular cylinders consisting of gyromagnetic uniaxial chiral media.

The geometrical configuration of the cross section and symbols used here are illustrated in Figure 3, where the constitutive relations for

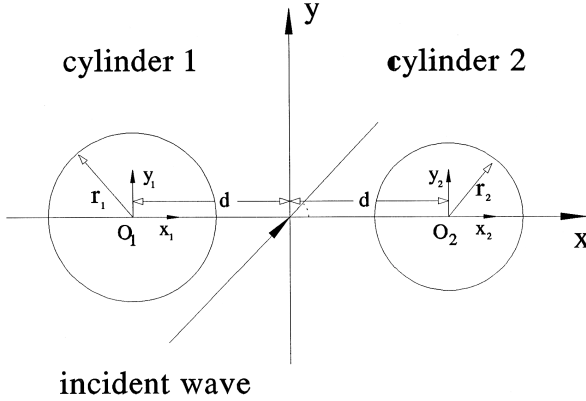


Figure 3. Geometry configuration of the structure of two circular cylinders.

cylinder j ($j = 1, 2$) are

$$\bar{D} = \bar{\epsilon}_j \cdot \bar{E} - \bar{\xi}_j \cdot \bar{H} \tag{21a}$$

$$\bar{B} = \bar{\mu}_j \cdot \bar{H} + \bar{\xi}_j \cdot \bar{E} \tag{21b}$$

The normally incident plane wave of unit amplitude of electric field with an incident angle φ^{inc} with respect to the $+x$ axis can be expanded in terms of the cylindrical vector wave functions:

$$\bar{E}^{inc}(\bar{r}) = \sum_{n=-\infty}^{\infty} (-i)^n [a_n^{inc} \bar{M}_n^{(1)}(k_0, \bar{r}) + b_n^{inc} \bar{N}_n^{(1)}(k_0, \bar{r})] \tag{22a}$$

$$\bar{H}^{inc}(\bar{r}) = \frac{k_0}{i\omega\mu_0} \sum_{n=-\infty}^{\infty} (-i)^n [a_n^{inc} \bar{N}_n^{(1)}(k_0, \bar{r}) + b_n^{inc} \bar{M}_n^{(1)}(k_0, \bar{r})] \tag{22b}$$

where $k_z = 0$ in the vector wave functions has been suppressed, and the coordinate system in which the vector wave functions are used has been indicated by the position vector in the vector wave functions. For the TM_z polarized incident plane wave, $a_n^{inc} = 0$, and $b_n^{inc} = e^{-in\varphi^{inc}}/k_0$. For the TE_z polarized incident plane wave, $a_n^{inc} = e^{-in\varphi^{inc}}/k_0$, and $b_n^{inc} = 0$.

The electromagnetic fields inside the scatterers can be separately expanded in terms of the cylindrical vector wave functions in the local coordinate systems:

$$\begin{aligned} \overline{E}_j^{int}(\overline{r}_j) = & \sum_{q=1}^2 \sum_{n=-\infty}^{\infty} (-i)^n \left\{ h_{qn}^{(j)} [A_q^{e(j)} \overline{M}_n^{(1)}(k_{\rho q}^{(j)}, \overline{r}_j) \right. \\ & \left. + B_q^{e(j)} \overline{N}_n^{(1)}(k_{\rho q}^{(j)}, \overline{r}_j) + C_q^{e(j)} \overline{L}_n^{(1)}(k_{\rho q}^{(j)}, \overline{r}_j)] \right\} \quad (23a) \end{aligned}$$

$$\begin{aligned} \overline{H}_j^{int}(\overline{r}_j) = & \sum_{q=1}^2 \sum_{n=-\infty}^{\infty} (-i)^n \left\{ h_{qn}^{(j)} [A_q^{h(j)} \overline{M}_n^{(1)}(k_{\rho q}^{(j)}, \overline{r}_j) \right. \\ & \left. + B_q^{h(j)} \overline{N}_n^{(1)}(k_{\rho q}^{(j)}, \overline{r}_j) + C_q^{h(j)} \overline{L}_n^{(1)}(k_{\rho q}^{(j)}, \overline{r}_j)] \right\} \quad (23b) \end{aligned}$$

for $j = 1, 2$. Here, $k_z = 0$ in the weighted coefficients of the vector wave functions has been suppressed.

The scattered fields are the superposition of those scattered from each cylinder

$$\overline{E}^{sca} = \sum_{j=1}^2 \overline{E}_j^{sca}, \quad \overline{H}^{sca} = \sum_{j=1}^2 \overline{H}_j^{sca} \quad (24)$$

where \overline{E}_j^{sca} and \overline{H}_j^{sca} can be represented in the O_j coordinate system as:

$$\overline{E}_j^{sca}(\overline{r}_j) = \sum_{n=-\infty}^{\infty} (-i)^n [a_n^{(j)} \overline{M}_n^{(4)}(k_0, \overline{r}_j) + b_n^{(j)} \overline{N}_n^{(4)}(k_0, \overline{r}_j)] \quad (25a)$$

$$\overline{H}_j^{sca}(\overline{r}_j) = \frac{k_0}{i\omega\mu_0} \sum_{n=-\infty}^{\infty} (-i)^n [a_n^{(j)} \overline{N}_n^{(4)}(k_0, \overline{r}_j) + b_n^{(j)} \overline{M}_n^{(4)}(k_0, \overline{r}_j)] \quad (25b)$$

Based on the addition theorem for the Bessel and Hankel functions [4, 22], the transformation of the cylindrical vector wave functions from the O_q coordinate to O_p coordinate are obtained:

$$\overline{Q}_n^{(1)}(k, \overline{r}_q) = \sum_{m=-\infty}^{\infty} \overline{Q}_m^{(1)}(k, \overline{r}_p) J_{m-n}(kd_{pq}) e^{i(m-n)\varphi_{pq}} \quad (26a)$$

$$\bar{Q}_n^{(4)}(k, \bar{r}_q) = \sum_{m=-\infty}^{\infty} \bar{Q}_m^{(1)}(k, \bar{r}_p) H_{m-n}^{(2)}(kd_{pq}) e^{i(m-n)\varphi_{pq}} \quad (26b)$$

where $\bar{Q} = \bar{M}$, or \bar{N} , (d_{pq}, φ_{pq}) is the position of O_q in the O_p coordinate system.

Using the addition theorem of the cylindrical vector wave functions and applying the boundary conditions at each surface of the scatterer to ensure the tangential components of electric and magnetic fields are continuous, a set of coupled linear equations involving the scattering coefficients are obtained. For the sake of consistency, details for the formulations of the solution procedure are organized in Appendix E.

The bistatic echo width of the scattering structure can be obtained by using the asymptotic expansion of Hankel function Eq. (16) and $\rho_{1,2} \approx \rho \pm d \cos \phi$ for $\rho \rightarrow \infty$, which result in

$$A_\sigma = 4k_0 \left| \sum_{n=-\infty}^{\infty} e^{-in\phi} (e^{-ik_0 d \cos \phi} b_n^{(1)} + e^{ik_0 d \cos \phi} b_n^{(2)}) \right|^2 + 4k_0 \left| \sum_{n=-\infty}^{\infty} e^{-in\phi} (e^{-ik_0 d \cos \phi} a_n^{(1)} + e^{ik_0 d \cos \phi} a_n^{(2)}) \right|^2 \quad (27)$$

For a TM_z polarized incident plane wave, the first term in the right-hand of (27) represents the copolarized echo width, while the second the crosspolarized one. For a TE_z polarized incident plane wave, the first and second terms in (27) stand for the cross- and copolarized echo width, respectively.

Again, it is important to examine the convergence properties of the final results for the series involved in the scattering by two circular cylinders of gyromagnetic uniaxial chiral media. Tables 3 and 4 present the numerical results for the convergence test of this scattering structure. It is seen that for proper truncated number N , reliable results can be obtained for all scattering angles. The convergence check indicates that the present cylindrical vector wave functions can be reliably applied to study the two-dimensional multiple-body problem of gyromagnetic uniaxial chiral media. To provide criteria for future references, Figures 4 and 5 illustrate the bistatic echo width of two circular cylinders of gyromagnetic uniaxial chiral media for TM_z and TE_z polarized incident wave, respectively.

A_σ/λ_0 (dB)	$\phi = 0^\circ$	$\phi = 45^\circ$	$\phi = 90^\circ$
$N = 3$	0.21751 <i>D</i> + 02	0.15329 <i>D</i> + 02	0.35310 <i>D</i> + 01
$N = 4$	0.21150 <i>D</i> + 02	0.15588 <i>D</i> + 02	0.70552 <i>D</i> + 01
$N = 5$	0.20822 <i>D</i> + 02	0.16497 <i>D</i> + 02	0.75536 <i>D</i> + 01
$N = 6$	0.20665 <i>D</i> + 02	0.16412 <i>D</i> + 02	0.70251 <i>D</i> + 01
$N = 7$	0.20665 <i>D</i> + 02	0.16418 <i>D</i> + 02	0.70255 <i>D</i> + 01
$N = 8$	0.20665 <i>D</i> + 02	0.16419 <i>D</i> + 02	0.70289 <i>D</i> + 01
$N = 9$	0.20665 <i>D</i> + 02	0.16419 <i>D</i> + 02	0.70294 <i>D</i> + 01
$N = 10$	0.20665 <i>D</i> + 02	0.16419 <i>D</i> + 02	0.70294 <i>D</i> + 01
A_σ/λ_0 (dB)	$\phi = 135^\circ$		$\phi = 180^\circ$
$N = 3$	0.21553 <i>D</i> + 02		0.12551 <i>D</i> + 02
$N = 4$	0.22033 <i>D</i> + 02		0.10885 <i>D</i> + 02
$N = 5$	0.21974 <i>D</i> + 02		0.11983 <i>D</i> + 02
$N = 6$	0.22115 <i>D</i> + 02		0.12469 <i>D</i> + 02
$N = 7$	0.22112 <i>D</i> + 02		0.12449 <i>D</i> + 02
$N = 8$	0.22112 <i>D</i> + 02		0.12449 <i>D</i> + 02
$N = 9$	0.22112 <i>D</i> + 02		0.12449 <i>D</i> + 02
$N = 10$	0.22112 <i>D</i> + 02		0.12449 <i>D</i> + 02

Table 3. Convergence test of two circular cylinders due to a TM_z polarized incident plane wave. The constitutive parameters of the media are taken to be as $\mu_t^{(1)}/\mu_0 = 1.3$, $\mu_z^{(1)}/\mu_0 = 1.4$, $g^{(1)}/\mu_0 = 0.08$, $\varepsilon_t^{(1)}/\varepsilon_0 = 2.7$, $\varepsilon_z^{(1)}/\varepsilon_0 = 2.5$, $\alpha^{(1)} = 0.3$, and $\gamma^{(1)} = 0.4$; and $\mu_t^{(2)}/\mu_0 = 1.8$, $\mu_z^{(2)}/\mu_0 = 1.2$, $g^{(2)}/\mu_0 = 0.12$, $\varepsilon_t^{(2)}/\varepsilon_0 = 2.5$, $\varepsilon_z^{(2)}/\varepsilon_0 = 2.1$, $\alpha^{(2)} = 0.3$, and $\gamma^{(2)} = 0.7$. The geometry parameters of the scatterer are taken to be $a_1 = 0.4\lambda_0$, $a_2 = 0.7\lambda_0$, and $d = 1.3\lambda_0$. The incident angle is 37° .

4. CONCLUDING REMARKS

In the present investigation, cylindrical vector wave functions are developed to represent the electromagnetic field in the source-free gyromagnetic uniaxial chiral medium. The formulation is greatly facilitated

A_σ/λ_0 (dB)	$\phi = 0^\circ$	$\phi = 45^\circ$	$\phi = 90^\circ$
$N = 3$	$0.23706D + 02$	$0.25522D + 02$	$0.23574D + 02$
$N = 4$	$0.20046D + 02$	$0.30209D + 02$	$0.29419D + 02$
$N = 5$	$0.19512D + 02$	$0.30377D + 02$	$0.29146D + 02$
$N = 6$	$0.19646D + 02$	$0.30228D + 02$	$0.29521D + 02$
$N = 7$	$0.19648D + 02$	$0.30224D + 02$	$0.29525D + 02$
$N = 8$	$0.19649D + 02$	$0.30223D + 02$	$0.29526D + 02$
$N = 9$	$0.19649D + 02$	$0.30223D + 02$	$0.29526D + 02$
$N = 10$	$0.19649D + 02$	$0.30223D + 02$	$0.29526D + 02$
A_σ/λ_0 (dB)	$\phi = 135^\circ$		$\phi = 180^\circ$
$N = 3$	$0.22589D + 02$		$0.25168D + 02$
$N = 4$	$0.24400D + 02$		$0.13815D + 02$
$N = 5$	$0.24120D + 02$		$0.15274D + 02$
$N = 6$	$0.24143D + 02$		$0.15804D + 02$
$N = 7$	$0.24140D + 02$		$0.15799D + 02$
$N = 8$	$0.24140D + 02$		$0.15799D + 02$
$N = 9$	$0.24140D + 02$		$0.15799D + 02$
$N = 10$	$0.24140D + 02$		$0.15799D + 02$

Table 4. Convergence test of two circular cylinders due to a TE_z polarized incident plane wave. The geometrical and constitutive parameters of the coating are taken to be the same as those of Table 3. The incident angle is 53° .

by using the concept of characteristic waves and the method of angular spectral expansion [21]. The formulation developed here generalizes the canonical solutions of vector wave functions for isotropic media, and recovers the case of the transversely chiral uniaxial bianisotropic medium [16], the uniaxial chiral medium [17], and the chiroferrite medium [18]. For applications of the cylindrical vector wave functions, an extended mode-matching method is proposed to study the two-dimensional electromagnetic scattering of a gyromagnetic uniaxial chiral cylinder with arbitrary cross section and a conducting circular cylinder with an inhomogeneous coating thickness of gyromagnetic uniaxial chiral medium. To check the convergence of the present cylindrical vector wave functions for nontrivial problems (such as the multiple-body problems), electromagnetic scattering by two circular cylinders of gyromagnetic

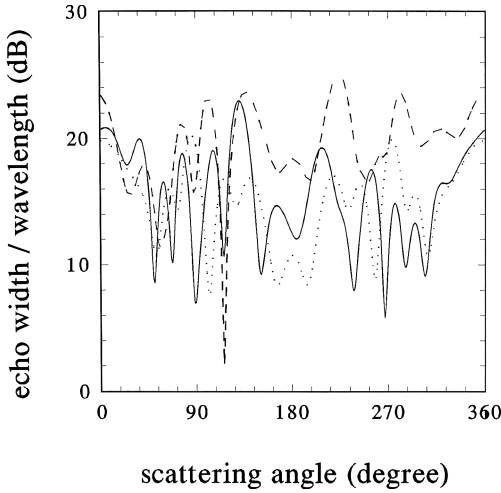


Figure 4. Scattering pattern of two circular cylinders, due to a normally incident TM_z polarized plane wave. The geometrical and constitutive parameters of the cylinders are taken to be the same as those of Table 3. The dotted line corresponds to the case of $\varphi^{inc} = 0^\circ$, the dashed line for $\varphi^{inc} = 90^\circ$, and the solid line for $\varphi^{inc} = 37^\circ$.

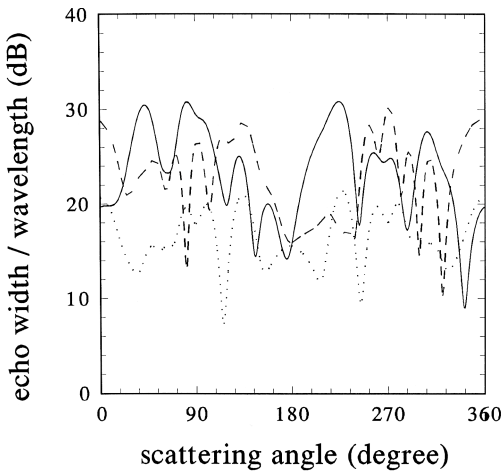


Figure 5. Scattering pattern of two circular cylinders, due to a normally incident TE_z polarized plane wave. The geometrical and constitutive parameters of the scatterers are taken to be the same as those of Table 3. The dotted line corresponds to the case of $\varphi^{inc} = 0^\circ$, the dashed line for $\varphi^{inc} = 90^\circ$, and the solid line for $\varphi^{inc} = 53^\circ$.

uniaxial chiral media is also investigated. Excellent convergence properties of the cylindrical vector wave functions in these application examples are numerically verified, which establishes the reliability and applicability of the present theory. It should be pointed out that the extended mode-matching method presented here, although does not require the eigenfunction expansion of Green dyadic, is only applicable to small aspect-ratio scatterers as the conventional T-matrix method. For scatterers of large aspect ratio scatterer, the challenge of convergence and time-consuming must be taken into account. However, this method is obviously superior to the conventional mode-matching method [8, 22] which can only be applicable to circular cylindrical structure, perturbation method [9] which is only suitable to near-circular cylindrical structure, T-matrix method [10] and multipole technique [12] both of which require the knowledge of source-incorporated solution, and may be regarded as the modified form of point-matching method [11] due to the same condition under which they can be utilized and the same challenge they will face up with for complex structure. Using the addition theorem of the cylindrical vector wave functions and the formulations for single scatterer, a homogenization theory [23] for the gyromagnetic uniaxial chiral composite media may be established, where the pair distributed function [24] can result from experiment, theoretical investigation, or numerical results. It is of interest to note that the cylindrical vector wave functions can be expanded as discrete sums of the spherical vector wave functions [25], therefore the present strategy could be extended to solve the problems of three-dimensional finite-domain structures. Noting the fact that the cylindrical functions can be expanded in terms of the plane wave functions [26], the present vector wave functions may also be applied to tackle the electromagnetic boundary-value problems involving the planar and curved surfaces of the gyromagnetic uniaxial chiral medium. Although excellent convergence and efficiency of the present cylindrical vector wave functions in tackling the two-dimensional physical phenomena have been demonstrated by extensive numerical computation, one should carefully examine the convergence and efficiency of the theory in actual computation when using the spherical or planar vector wave functions for three-dimensional finite-domain or planar-curved-surface electromagnetic phenomena associated with the gyromagnetic uniaxial chiral medium. Nevertheless, it is believed that the present cylindrical vector wave functions and the generalized mode-matching method would

be helpful in analyzing and exploiting the physical phenomena associated with the boundary-value problems of layered structures as well as multi-scatterers consisting of gyromagnetic uniaxial chiral media.

APPENDIX A: DETAIL OF THE VECTOR WAVE FUNCTIONS

Substituting the expressions (4) and (6b) in (6a), we have the magnetic field expanded in terms of the eigenvectors in a circular cylindrical coordinate system

$$\begin{aligned} \overline{H}(\vec{r}) = & \sum_{q=1}^2 \int_{-\infty}^{\infty} dk_z \sum_{n=-\infty}^{\infty} h_{qn}(k_z) \int_{\phi_k=0}^{2\pi} d\phi_k e^{-i[k_z z + k_{\rho q} \rho \cos(\phi - \phi_k) + n\phi_k]} \\ & \cdot \{ [A_q(k_z) \cos(\phi - \phi_k) + B_q(k_z) \sin(\phi - \phi_k)] \bar{e}_\rho \\ & + [-A_q(k_z) \sin(\phi - \phi_k) + B_q(k_z) \cos(\phi - \phi_k)] \bar{e}_\phi + \bar{e}_z \} \end{aligned} \quad (\text{A1})$$

Noting the well-known identity [2,3]

$$e^{-ik_{\rho q} \rho \cos(\phi - \phi_k)} = \sum_{m=-\infty}^{\infty} (-i)^m J_m(k_{\rho q} \rho) e^{-im(\phi - \phi_k)} \quad (\text{A2})$$

and taking the derivatives of (A2) with respect to ρ and ϕ , respectively, we have

$$\cos(\phi - \phi_k) e^{-ik_{\rho q} \rho \cos(\phi - \phi_k)} = \sum_{m=-\infty}^{\infty} (-i)^{m-1} \frac{\partial J_m(k_{\rho q} \rho)}{k_{\rho q} \partial \rho} e^{-im(\phi - \phi_k)} \quad (\text{A3})$$

and

$$\sin(\phi - \phi_k) e^{-ik_{\rho q} \rho \cos(\phi - \phi_k)} = - \sum_{m=-\infty}^{\infty} (-i)^m \frac{m J_m(k_{\rho q} \rho)}{k_{\rho q} \rho} e^{-im(\phi - \phi_k)} \quad (\text{A4})$$

Inserting Eqs. (A2–A4) into equation (A1), we obtain

$$\overline{H}(\vec{r}) = \sum_{q=1}^2 \int_{-\infty}^{\infty} dk_z \sum_{n=-\infty}^{\infty} h_{qn}(k_z) [P_n(k_z) \bar{e}_\rho + Q_n(k_z) \bar{e}_\phi + R_n(k_z) \bar{e}_z] \quad (\text{A5})$$

where

$$\begin{aligned}
 P_n(k_z) &= \int_{\phi_k=0}^{2\pi} d\phi_k \sum_{m=-\infty}^{\infty} \left[(-i)^{m-1} \frac{\partial J_m(k_{\rho q} \rho)}{k_{\rho q} \partial \rho} A_q(k_z) \right. \\
 &\quad \left. - (-i)^m \frac{m J_m(k_{\rho q} \rho)}{k_{\rho q} \rho} B_q(k_z) \right] e^{-i(k_z z + m\phi) + i(m-n)\phi_k} \\
 &= 2\pi (-i)^n \left[\frac{i \partial J_n(k_{\rho q} \rho) A_q(k_z)}{k_{\rho q} \partial \rho} - \frac{n J_n(k_{\rho q} \rho) B_q(k_z)}{k_{\rho q} \rho} \right] e^{-i(k_z z + n\phi)}
 \end{aligned} \tag{A6}$$

$$\begin{aligned}
 Q_n(k_z) &= \int_{\phi_k=0}^{2\pi} d\phi_k \sum_{m=-\infty}^{\infty} \left[(-i)^{m-1} \frac{\partial J_m(k_{\rho q} \rho)}{k_{\rho q} \partial \rho} B_q(k_z) \right. \\
 &\quad \left. + (-i)^m \frac{m J_m(k_{\rho q} \rho)}{k_{\rho q} \rho} A_q(k_z) \right] e^{-i(k_z z + m\phi) + i(m-n)\phi_k} \\
 &= 2\pi (-i)^n \left[\frac{i \partial J_n(k_{\rho q} \rho) B_q(k_z)}{k_{\rho q} \partial \rho} - \frac{n J_n(k_{\rho q} \rho) A_q(k_z)}{k_{\rho q} \rho} \right] e^{-i(k_z z + n\phi)}
 \end{aligned} \tag{A7}$$

and

$$\begin{aligned}
 R_n(k_z) &= \int_{\phi_k=0}^{2\pi} d\phi_k \sum_{m=-\infty}^{\infty} [(-i)^m J_m(k_{\rho q} \rho)] e^{-i(k_z z + m\phi) + i(m-n)\phi_k} \\
 &= 2\pi (-i)^n J_n(k_{\rho q} \rho) e^{-i(k_z z + n\phi)}
 \end{aligned} \tag{A8}$$

By introducing the cylindrical vector wave functions (8a)–(8c) and recalling the complete property of this set of functions [2,4,22], it is reasonable to assume the magnetic field in gyromagnetic uniaxial chiral medium can be represented in the form of (7). Then, comparing the coordinate components of (7) with those of (A5) where $P_n(k_z)$, $Q_n(k_z)$ and $R_n(k_z)$ are determined by (A6)–(A8), we derive a set of equations

$$A_q^h(k_z) = -\frac{2i}{k_{\rho q}} B_q(k_z) \tag{A9}$$

$$\frac{k_z}{k_q} B_q^h(k_z) + i C_q^h(k_z) = -\frac{2}{k_{\rho q}} A_q(k_z) \tag{A10}$$

and

$$\frac{k_{\rho q}^2}{k_q} B_q^h(k_z) - i k_z C_q^h(k_z) = 2 \tag{A11}$$

The solutions to this set of linear equations (A9)–(A11) result in the expressions of (9a)–(9c).

APPENDIX B: DETAILED PROCEDURE FOR THE SOLUTIONS OF EQS. (14a–14d)

For simplicity, we introduce

$$V_{qn}^p(\rho) = -\frac{in}{\rho} J_n(k_{\rho q}\rho) C_q^p(k_z = 0) - k_{\rho q} J_n'(k_{\rho q}\rho) A_q^p(k_z = 0) \quad (\text{B1})$$

$$X_{qn}^p(\rho) = k_{\rho q} J_n(k_{\rho q}\rho) B_q^p(k_z = 0) \quad (\text{B2})$$

$$Y_{qn}^p(\rho) = -\frac{in}{\rho} J_n(k_{\rho q}\rho) A_q^p(k_z = 0) + k_{\rho q} J_n'(k_{\rho q}\rho) C_q^p(k_z = 0) \quad (\text{B3})$$

where $\rho = f(\phi)$, $q = 1, 2$ and $p = e, h$.

Multiplying both sides of Eqs. (14a–14d) with $e^{im\phi}$ ($m = -N, -N + 1, \dots, N - 1, N$) and integrating with respect of ϕ from 0 to 2π , we end up with

$$\sum_{q=1}^2 [I^{qe}] [\bar{h}_q] = [I^{(2)}] [\bar{a}] \quad (\text{B4})$$

$$\sum_{q=1}^2 [A^{qh}] [\bar{h}_q] = -\frac{k_0}{i\omega\mu_0} [I^{(5)}] [\bar{a}] \quad (\text{B5})$$

$$\sum_{q=1}^2 [I^{qh}] [\bar{h}_q] + \frac{k_0}{i\omega\mu_0} [I^{(2)}] [\bar{b}] = [P] [\bar{I}] \quad (\text{B6})$$

$$\sum_{q=1}^2 [A^{qe}] [\bar{h}_q] - [I^{(5)}] [\bar{b}] = [Q] [\bar{I}] \quad (\text{B7})$$

where $[\bar{a}]$ and $[\bar{b}]$ are column vectors of the expansion coefficients of the scattered waves, respectively, and

$$(I^{qp})_{mn} = \int_{\phi=0}^{2\pi} (-i)^{n'} e^{-i(n'-m')\phi} [Y_{qn'}^p(\rho) \sin \theta + V_{qn'}^p(\rho) \cos \theta] d\phi \quad (\text{B8})$$

$$(I^{(2)})_{mn} = \int_{\phi=0}^{2\pi} (-i)^{n'} e^{-i(n'-m')\phi} \begin{bmatrix} -\frac{in'}{\rho} H_{n'}^{(2)}(k_0\rho) \sin \theta \\ -k_0 H_{n'}^{(2)'}(k_0\rho) \cos \theta \end{bmatrix} d\phi \quad (\text{B9})$$

$$(P)_{nm} = \frac{1}{i\omega\mu_0} \int_{\phi=0}^{2\pi} (-i)^{n'} e^{-i(n'-m')\phi} \begin{bmatrix} \frac{in}{\rho} J_{n'}(k_0\rho) \sin\theta \\ + k_0 J'_{n'}(k_0\rho) \cos\theta \end{bmatrix} d\phi \quad (\text{B10})$$

$$(Q)_{nm} = \int_{\theta=0}^{2\pi} (-i)^{n'} e^{-i(n'-m')\phi} J_{n'}(k_0\rho) d\phi \quad (\text{B11})$$

$$(A^{qp})_{mn} = \int_{\phi=0}^{2\pi} (-i)^{n'} e^{-i(n'-m')\phi} X_{qn'}^p(\rho) d\phi \quad (\text{B12})$$

$$(I^{(5)})_{mn} = \int_{\phi=0}^{2\pi} (-i)^{n'} e^{-i(n'-m')\phi} k_0 H_{n'}^{(2)}(k_0\rho) d\phi \quad (\text{B13})$$

for $q = 1$ or 2 , $p = e$ or h , $m, n \in [1, 2N+1]$ and $m' = m - (N+1)$, $n' = n - (N+1)$. Here, $[\bar{I}]$ is the $(2N+1)$ dimension unit vector, and the primes over the Bessel and Hankel functions denote the derivatives with respect to the arguments.

Straightforward algebraic manipulation for (B4)–(B7), we obtain

$$\begin{aligned} [\bar{a}] &= \left[\frac{i\omega\mu_0}{k_0} [I^{(2)}]^{-1} [D^{(1)}] + [I^{(5)}]^{-1} [D^{(2)}] \right]^{-1} \\ &\quad \cdot \left[\frac{i\omega\mu_0}{k_0} [I^{(2)}]^{-1} [P] + [I^{(5)}]^{-1} [Q] \right] \cdot [\bar{I}] \end{aligned} \quad (\text{B14})$$

$$\begin{aligned} [\bar{b}] &= \left[\frac{k_0}{i\omega\mu_0} [D^{(1)}]^{-1} [I^{(2)}] + [D^{(2)}]^{-1} [I^{(5)}] \right]^{-1} \\ &\quad \cdot \left[[D^{(1)}]^{-1} [P] - [D^{(2)}]^{-1} [Q] \right] \cdot [\bar{I}] \end{aligned} \quad (\text{B15})$$

where

$$[D^{(1)}] = [I^{1h}][C^{(2)}] + [I^{2h}][C^{(1)}] \quad (\text{B16})$$

$$[D^{(2)}] = [A^{1e}][C^{(2)}] + [A^{2h}][C^{(1)}] \quad (\text{B17})$$

and

$$\begin{aligned} [C^{(1)}] &= \left[[I^{1e}]^{-1} [I^{2e}] - [A^{1h}]^{-1} [A^{2h}] \right]^{-1} \\ &\quad \cdot \left[[I^{1e}]^{-1} [I^{(2)}] + \frac{k_0}{i\omega\mu_0} [A^{1h}]^{-1} [I^{(5)}] \right] \end{aligned} \quad (\text{B18})$$

$$[C^{(2)}] = \left[[I^{2e}]^{-1} [I^{1e}] - [A^{2h}]^{-1} [A^{1h}] \right]^{-1} \cdot \left[[I^{2e}]^{-1} [I^{(2)}] + \frac{k_0}{i\omega\mu_0} [A^{2h}]^{-1} [I^{(5)}] \right] \quad (\text{B19})$$

After numerically evaluating the matrices involved, equations (B14) and (B15) would result in the expansion coefficients of the scattered fields.

APPENDIX C: ELECTROMAGNETIC SCATTERING BY A GYROMAGNETIC UNIAXIAL CHIRAL CIRCULAR CYLINDER

Here, we will present the explicit expressions of expansion coefficients of the scattered field for the scattering of a gyromagnetic uniaxial chiral circular cylinder of radius ρ_0 . In the case of a TM_z polarized incident plane wave illuminating along the $+x$ axis, the incident electromagnetic fields can be expanded in terms of the circular cylindrical vector wave functions, as presented in Eqs. (12a) and (12b). The electromagnetic fields excited inside the scatterer can be represented in terms of the cylindrical vector wave functions in the way we have presented in Sec. 2. And the scattered electromagnetic waves may have TM_z and TE_z components and should be expanded as Eqs. (13a) and (13b).

Applying the widely-employed mode matching method [8,22] to have the boundary conditions of continuous tangential electric and magnetic fields satisfied at the outer surface of the scatterer $\rho = \rho_0$, the expansion coefficients of the scattered fields are derived as

$$a_n = -\frac{2}{\pi\eta_0\rho_0\Delta_n(\rho_0)}\delta(k_z) \left[V_{1n}^e(\rho_0)X_{2n}^h(\rho_0) - V_{2n}^e(\rho_0)X_{1n}^h(\rho_0) \right] \quad (\text{C1})$$

and

$$b_n = \frac{1}{\Delta_n(\rho_0)}\delta(k_z) \left[J_n(k_0\rho_0)C_n\rho_0 + \frac{i}{\eta_0}J'_n(k_0\rho_0)D_n(\rho_0) \right] \quad (\text{C2})$$

where

$$V_{qn}^p(\rho_0) = A_q^p(k_z)k_{\rho q}J'_n(k_{\rho q}\rho_0) + \frac{in}{\rho_0}C_q^p(k_z)J_n(k_{\rho q}\rho_0) \quad (\text{C3})$$

$$X_{qn}^p(\rho_0) = B_q^p(k_z)k_{\rho q}J_n(k_{\rho q}\rho_0) \quad (\text{C4})$$

for $q = 1, 2$ and $p = e, h$. In Eqs. (C1) and (C2),

$$C_n(\rho_0) = -k_0 H_n^{(2)'}(k_0 \rho_0) [V_{1n}^h(\rho_0) X_{2n}^h(\rho_0) - V_{2n}^h(\rho_0) X_{1n}^h(\rho_0)] \\ - i\omega \varepsilon_0 H_n^{(2)}(k_0 \rho_0) [V_{1n}^e(\rho_0) V_{2n}^h(\rho_0) - V_{2n}^e(\rho_0) V_{1n}^h(\rho_0)] \quad (\text{C5})$$

$$\Delta_n(\rho_0) = -k_0 H_n^{(2)}(k_0 \rho_0) C_n(\rho_0) - i\omega \varepsilon_0 H_n^{(2)'}(k_0 \rho_0) D_n(\rho_0) \quad (\text{C6})$$

$$D_n(\rho_0) = k_0 H_n^{(2)'}(k_0 \rho_0) [X_{1n}^e(\rho_0) X_{2n}^h(\rho_0) - X_{2n}^e(\rho_0) X_{1n}^h(\rho_0)] \\ + i\omega \varepsilon_0 H_n^{(2)}(k_0 \rho_0) [V_{1n}^e(\rho_0) X_{2n}^e(\rho_0) - V_{2n}^e(\rho_0) X_{1n}^e(\rho_0)] \quad (\text{C7})$$

Due to the emergence of Dirac delta function $\delta(k_z)$ in (C1) and (C2), the infinite integration of the k_z variable for the scattered fields has actually disappeared. using the asymptotic expression of the Hankel function in the far region Eq. (22), the bistatic echo width of this structure Eq. (21) can be rewritten in a more explicit form

$$A_\sigma(\phi) = 4k_0 \left[\left| \sum_{n=0}^{\infty} (-1)^n \delta_n a_n \cos(n\phi) \right|^2 + \left| \sum_{n=0}^{\infty} (-1)^n \delta_n b_n \cos(n\phi) \right|^2 \right] \quad (\text{C8})$$

where δ_n is the Neumann factor, i.e., $\delta_n = 1$ for $n = 0$ and 2 for $n > 0$.

APPENDIX D: SOLUTIONS FOR SCATTERING COEFFICIENTS OF A CONDUCTING CIRCULAR CYLINDER WITH AN INHOMOGENEOUS COATING THICKNESS OF GYROMAGNETIC UNIAXIAL CHIRAL MEDIUM

For simplicity, we introduce

$$V_{qn}^{p(j)}(\rho) = -\frac{in}{\rho} Z_n^{(j)}(k_{\rho q} \rho) C_q^p(k_z = 0) - k_{\rho q} Z_n^{(j)'}(k_{\rho q} \rho) A_q^p(k_z = 0) \quad (\text{D1})$$

$$X_{qn}^{p(j)}(\rho) = k_{\rho q} Z_n^{(j)}(k_{\rho q} \rho) B_q^p(k_z = 0) \quad (\text{D2})$$

$$Y_{qn}^{p(j)}(\rho) = -\frac{in}{\rho} Z_n^{(j)}(k_{\rho q} \rho) A_q^p(k_z = 0) + k_{\rho q} Z_n^{(j)'}(k_{\rho q} \rho) C_q^p(k_z = 0) \quad (\text{D3})$$

where $\rho = f(\phi)$ or $\rho = a$, $q = 1$ or 2, $p = e$ or h , and $Z_n^{(j)}(\cdot) = J_n(\cdot)$ or $Z_n^{(j)}(\cdot) = H_n^{(2)}(\cdot)$ for $j = 1, 4$, respectively.

From the boundary conditions Eqs. (19a) and (19b) at $\rho = a$, we have

$$[\bar{h}_1^{(4)}] = [A^{11}][\bar{h}_1^{(1)}] + [A^{12}][\bar{h}_2^{(1)}] \quad (\text{D4})$$

$$[\bar{h}_2^{(4)}] = [A^{21}][\bar{h}_1^{(1)}] + [A^{22}][\bar{h}_2^{(1)}] \quad (\text{D5})$$

where

$$[A^{11}] = \left[[X^{2(4)}]^{-1}[X^{1(4)}] - [V^{2(4)}]^{-1}[V^{1(4)}] \right]^{-1} \cdot \left[[V^{2(4)}]^{-1}[V^{1(1)}] - [X^{2(4)}]^{-1}[X^{1(1)}] \right] \quad (\text{D6})$$

$$[A^{12}] = \left[[X^{2(4)}]^{-1}[X^{1(4)}] - [V^{2(4)}]^{-1}[V^{1(4)}] \right]^{-1} \cdot \left[[V^{2(4)}]^{-1}[V^{2(1)}] - [X^{2(4)}]^{-1}[X^{2(1)}] \right] \quad (\text{D7})$$

$$[A^{21}] = \left[[X^{1(4)}]^{-1}[X^{2(4)}] - [V^{1(4)}]^{-1}[V^{2(4)}] \right]^{-1} \cdot \left[[V^{1(4)}]^{-1}[V^{1(1)}] - [X^{1(4)}]^{-1}[X^{1(1)}] \right] \quad (\text{D8})$$

$$[A^{22}] = \left[[X^{1(4)}]^{-1}[X^{2(4)}] - [V^{1(4)}]^{-1}[V^{2(4)}] \right]^{-1} \cdot \left[[V^{1(4)}]^{-1}[V^{2(1)}] - [X^{1(4)}]^{-1}[X^{2(1)}] \right] \quad (\text{D9})$$

and the matrices involved in Eqs. (D6)–(D9) are all diagonal with the diagonal elements given as

$$(X_p^{q(j)})_{mn} = X_{qn'}^{p(j)}(\rho = a)\delta(m' - n') \quad (\text{D10})$$

$$(V_p^{q(j)})_{mn} = V_{qn'}^{p(j)}(\rho = a)\delta(m' - n') \quad (\text{D11})$$

for $m, n \in [1, 2N + 1]$ and $m' = m - (N + 1), n' = n - (N + 1)$.

After substituting Eqs. (D4) and (D5) into Eqs. (20a)–(20d), multiplying both sides of the resulting equations with $e^{im\phi}$ ($m = -N, -N + 1, \dots, N - 1, N$) and integrating from 0 to 2π , we end up with

$$\sum_{q=1}^2 [I^{qe}] [\bar{h}_q^{(1)}] = [I^{(2)}] [\bar{a}] \quad (\text{D12})$$

$$\sum_{q=1}^2 [I^{qh}] [\bar{h}_q^{(1)}] + \frac{k_0}{i\omega\mu_0} [I^{(2)}] [\bar{b}] = [P] [\bar{I}] \quad (\text{D13})$$

$$\sum_{q=1}^2 [A^{qe}] [\bar{h}_q^{(1)}] - [I^{(5)}] [\bar{b}] = [Q] [\bar{I}] \quad (\text{D14})$$

$$\sum_{q=1}^2 [A^{qh}] [\bar{h}_q^{(1)}] = -\frac{k_0}{i\omega\mu_0} [I^{(5)}] [\bar{a}] \quad (\text{D15})$$

where

$$[I^{qp}] = [B_p^{q(1)}] + [B_p^{1(4)}][A^{1q}] + [B_p^{2(4)}][A^{2q}] \quad (\text{D16})$$

$$[A^{qp}] = [C_p^{q(1)}] + [C_p^{1(4)}][A^{1q}] + [C_p^{2(4)}][A^{2q}] \quad (\text{D17})$$

with

$$(B_p^{q(j)})_{mn} = \int_{\phi=0}^{2\pi} (-i)^{n'} e^{-i(n'-m')\phi} \cdot \left[Y_{qn'}^{p(j)}(\rho) \sin \theta + V_{qn'}^{p(j)}(\rho) \cos \theta \right] d\phi \quad (\text{D18})$$

$$(I^{(2)})_{mn} = \int_{\phi=0}^{2\pi} (-i)^{n'} e^{-i(n'-m')\phi} \cdot \left[-\frac{in'}{\rho} H_{n'}^{(1)}(k_0\rho) \sin \theta - k_0 H_{n'}^{(1)'}(k_0\rho) \cos \theta \right] d\phi \quad (\text{D19})$$

$$(P)_{nm} = \frac{1}{i\omega\mu_0} \int_{\phi=0}^{2\pi} (-i)^{n'} e^{-i(n'-m')\phi} \cdot \left[-\frac{in'}{\rho} J_{n'}(k_0\rho) \sin \theta - k_0 J_{n'}(k_0\rho) \cos \theta \right] d\phi \quad (\text{D20})$$

$$(Q)_{mn} = \int_{\phi=0}^{2\pi} (-i)^{n'} e^{-i(n'-m')\phi} J_{n'}(k_0\rho) d\phi \quad (\text{D21})$$

$$(C_p^{q(j)})_{mn} = \int_{\phi=0}^{2\pi} (-i)^{n'} e^{-i(n'-m')\phi} X_{qn'}^{p(j)}(\rho) d\phi \quad (\text{D22})$$

$$(I^{(5)})_{mn} = \int_{\phi=0}^{2\pi} (-i)^{n'} e^{-i(n'-m')\phi} k_0 H_{n'}^{(2)}(k_0\rho) d\phi \quad (\text{D23})$$

for $q = 1$ or 2 , and $p = e$ or h . Here, $[\bar{I}]$ is the $(2N+1)$ dimensional unit vector.

Straightforward algebraic manipulation for (D12)–(D15) yields

$$[\bar{a}] = \left[\frac{i\omega\mu_0}{k_0} [I^{(2)}]^{-1} [D^{(1)}] + [I^{(5)}]^{-1} [D^{(2)}] \right]^{-1}$$

$$\cdot \left[\frac{i\omega\mu_0}{k_0} [I^{(2)}]^{-1} [P] + [I^{(5)}]^{-1} [Q] \right] \cdot [\bar{I}] \quad (\text{D24})$$

$$\begin{aligned} [\bar{b}] = & \left[\frac{k_0}{i\omega\mu_0} [D^{(1)}]^{-1} [I^{(2)}] + [D^{(2)}]^{-1} [I^{(5)}] \right]^{-1} \\ & \cdot \left[[D^{(1)}]^{-1} [P] - [D^{(2)}]^{-1} [Q] \right] \cdot [\bar{I}] \end{aligned} \quad (\text{D25})$$

where

$$[D^{(1)}] = [I^{1h}][C^{(2)}] + [I^{2h}][C^{(1)}] \quad (\text{D26})$$

$$[D^{(2)}] = [A^{1e}][C^{(2)}] + [A^{2h}][C^{(1)}] \quad (\text{D27})$$

and

$$\begin{aligned} [C^{(1)}] = & \left[[I^{1e}]^{-1} [I^{(2e)}] - [A^{1h}]^{-1} [A^{2h}] \right]^{-1} \\ & \cdot \left[[I^{1e}]^{-1} [I^{(2)}] + \frac{k_0}{i\omega\mu_0} [A^{1h}]^{-1} [I^{(5)}] \right] \end{aligned} \quad (\text{D28})$$

$$\begin{aligned} [C^{(2)}] = & \left[[I^{2e}]^{-1} [I^{(1e)}] - [A^{2h}]^{-1} [A^{1h}] \right]^{-1} \\ & \cdot \left[[I^{2e}]^{-1} [I^{(2)}] + \frac{k_0}{i\omega\mu_0} [A^{2h}]^{-1} [I^{(5)}] \right] \end{aligned} \quad (\text{D29})$$

Equations (D24) and (D25) gives the complete solutions of the expansion coefficients of the scattered wave of the structure, which makes the bistatic echo width expression easily evaluated.

APPENDIX E: DETAILS FOR THE SCATTERING OF TWO GYROMAGNETIC UNIAXIAL CHIRAL CIRCULAR CYLINDERS

The boundary conditions at $\rho_1 = a_1$ can be written as

$$[A_1^{(1)}][\bar{a}^{inc}] + [B_1^{(1)}][\bar{a}^{(1)}] + [C_1^{(1)}][\bar{a}^{(2)}] = \sum_{q=1}^2 [D_q^{e(1)}][\bar{h}_q^{(1)}] \quad (\text{E1})$$

$$[A_1^{(1)}][\bar{b}^{inc}] + [B_1^{(1)}][\bar{b}^{(1)}] + [C_1^{(1)}][\bar{b}^{(2)}] = -\frac{i\omega\mu_0}{k_0} \sum_{q=1}^2 [D_q^{h(1)}][\bar{h}_q^{(1)}] \quad (\text{E2})$$

$$[A_2^{(1)}][\bar{a}^{inc}] + [B_2^{(1)}][\bar{a}^{(1)}] + [C_2^{(1)}][\bar{a}^{(2)}] = -\frac{i\omega\mu_0}{k_0} \sum_{q=1}^2 [E_q^{h(1)}][\bar{h}_q^{(1)}] \quad (\text{E3})$$

$$[A_2^{(1)}][\bar{b}^{inc}] + [B_2^{(1)}][\bar{b}^{(1)}] + [C_2^{(1)}][\bar{b}^{(2)}] = \sum_{q=1}^2 [E_q^{e(1)}][\bar{h}_q^{(1)}] \quad (\text{E4})$$

and the boundary conditions at $\rho_2 = a_2$ can be written as

$$[A_1^{(2)}][\bar{a}^{inc}] + [C_1^{(2)}][\bar{a}^{(1)}] + [B_1^{(2)}][\bar{a}^{(2)}] = \sum_{q=1}^2 [D_q^{e(2)}][\bar{h}_q^{(2)}] \quad (\text{E5})$$

$$[A_1^{(2)}][\bar{b}^{inc}] + [C_1^{(2)}][\bar{b}^{(1)}] + [B_1^{(2)}][\bar{b}^{(2)}] = -\frac{i\omega\mu_0}{k_0} \sum_{q=1}^2 [D_q^{h(2)}][\bar{h}_q^{(2)}] \quad (\text{E6})$$

$$[A_2^{(2)}][\bar{b}^{inc}] + [C_2^{(2)}][\bar{b}^{(1)}] + [B_2^{(2)}][\bar{b}^{(2)}] = \sum_{q=1}^2 [E_q^{e(2)}][\bar{h}_q^{(2)}] \quad (\text{E7})$$

$$[A_2^{(2)}][\bar{a}^{inc}] + [C_2^{(2)}][\bar{a}^{(1)}] + [B_2^{(2)}][\bar{a}^{(2)}] = -\frac{i\omega\mu_0}{k_0} \sum_{q=1}^2 [E_q^{h(2)}][\bar{h}_q^{(2)}] \quad (\text{E8})$$

where

$$(A_1^{(j)})_{mn} = (-i)^{n'} J_{m'-n'}(k_0 d) e^{i(m'-n')\phi_j} J'_{m'}(k_0 a_j) \quad (\text{E9})$$

$$(A_2^{(j)})_{mn} = (-i)^{n'} J_{m'-n'}(k_0 d) e^{i(m'-n')\phi_j} J_{m'}(k_0 a_j) \quad (\text{E10})$$

$$(B_1^{(j)})_{mn} = (-i)^{n'} H_{n'}^{(2)'}(k_0 a_j) \delta(m' - n') \quad (\text{E11})$$

$$(B_2^{(j)})_{mn} = (-i)^{n'} H_{n'}^{(2)}(k_0 a_j) \delta(m' - n') \quad (\text{E12})$$

$$(C_1^{(j)})_{mn} = (-i)^{n'} H_{m'-n'}^{(2)}(2k_0 d) e^{i(m'-n')\phi_j} J_{m'}(k_0 a_j) \quad (\text{E13})$$

$$(C_2^{(j)})_{mn} = (-i)^{n'} H_{m'-n'}^{(2)}(2k_0 d) e^{i(m'-n')\phi_j} J'_{m'}(k_0 a_j) \quad (\text{E14})$$

$$(E_q^{p(j)})_{mn} = \frac{(-i)^{n'}}{k_0} k_{\rho q}^{(j)}(k_{\rho q}^{(j)} a_j) B_q^{p(j)}(k_z = 0) \delta(m' - n') \quad (\text{E15})$$

$$(D_q^{p(j)})_{mn} = \frac{(-i)^{n'}}{k_0} \left[k_{\rho q}^{(j)} J'_{n'}(k_{\rho q}^{(j)} a_j) A_q^{p(j)}(k_z = 0) + \frac{in'}{\rho_j} J_{n'}(k_{\rho q}^{(j)} a_j) C_q^{p(j)}(k_z = 0) \right] \delta(m' - n') \quad (\text{E16})$$

with $\phi_1 = 0$, $\phi_2 = \pi$, $j = 1$ or 2 , $p = e$ or h , $m, n \in [1, 2N + 1]$ and $m' = m - (N + 1)$, $n' = n - (N + 1)$.

Straightforward manipulation for Eqs. (E1)–(E8) will give rise to the solutions of the scattering coefficient vectors $[\bar{a}^{(1)}]$, $[\bar{b}^{(1)}]$, and $[\bar{a}^{(2)}]$, $[\bar{b}^{(2)}]$, respectively.

REFERENCES

1. Hansen, W. W., "A new type of expansion in radiation problems," *Phys. Rev.*, Vol. 47, 139–143, 1935.
2. Morse, P. M., and H. Feshbach, *Methods of Theoretical Physics*, McGraw-Hill, New York, 1953.
3. Tai, C. T., *Dyadic Green's Functions in Electromagnetic Theory*, Intertext Publisher, New York, 1971.
4. Zhou, X. -S., *Vector Wave Functions in Electromagnetic Theory*, Roma, 1994.
5. Graglia, R. D., P. L. E. Uslenghi, and R. S. Zich, "Moment method with isoparametric elements for three-dimensional anisotropic scatterers," *Proc. IEEE*, Vol. 77, 750–760, 1989.
6. Varadan, V. V., A. Lakhtakia, and V. K. Varadan, "Scattering by a three dimensional anisotropic scatterers," *IEEE Trans. Antennas Propagat.*, Vol. 37, 800–802, 1989.
7. Papadakis, S. N., N. K. Uzunoglu, and N. Christos, "Scattering of a plane wave by a general anisotropic dielectric ellipsoid," *J. Opt. Soc. Am A*, Vol. 7, 991–997, 1990.
8. Kong, J. A., *Theory of Electromagnetic Waves*, Wiley, New York, 1975.
9. Yeh, C., "Perturbation method in the diffraction of electromagnetic waves by arbitrarily shaped penetrable obstacles," *J. Math. Phys.*, Vol. 6, 2008–2013, 1965.
10. Varadan, V. K., and V. V. Varadan, Ed., *Acoustic, Electromagnetic and Elastic Wave Scattering—Focus on the T-Matrix Approach*, Pergamon, New York, 1980.
11. Rothwell, E. J., and L. L. Frasc, "Propagation characteristics of dielectric-rod-loaded waveguides," *IEEE Trans. Microwave Theory Tech.*, Vol. 36, 594–600, 1988.
12. Hafner, C., *The Generalized Multipole Technique for Computational Electromagnetics*, Artech House, London, 1990.
13. Lindell, I. V., A. H. Sihvola, S. A. Tretyakov, and A. J. Viitanen, *Electromagnetic Waves in Chiral and Bianisotropic Media*, Artech House, Norwood, 1994.

14. Priou, A., Ed., *Bianisotropic and Biisotropic Media and Applications*, EMW Publisher, Boston, 1994.
15. Engheta, N., Ed., "Special Issue on wave Interaction with Chiral and Complex Material," *J. Electromagn. Waves Appl.*, Vol. 6, 537–793, 1992.
16. Lindell, I. V., A. J. Viitanen, and P. K. Koivisto, "Plane-wave propagation in transversely bianisotropic uniaxial medium," *Microwave Opt. Technol. Lett.*, Vol. 6, 478–481, 1993.
17. Lindell, I. V., and A. H. Sihvola, "Plane-wave reflection from uniaxial chiral interface and its application to polarization transformation," *IEEE Trans. Antennas Propagat.*, Vol. 43, 1397–1404, 1995.
18. Engheta, N., D. L. Jaggard, and M. W. Kowarz, "Electromagnetic waves in Faraday chiral media," *IEEE Trans. Antennas Propagat.*, Vol. 40, 367–373, 1992.
19. Post, E. J., *Formal Structures of Electromagnetics*, North-Holland, Amsterdam, 1962.
20. Chen, H. C., *Theory of Electromagnetic Waves—A Coordinate Free Approach*, McGraw-Hill, New York, 1983.
21. Uzunglu, N. K., P. G. Cottis, and J. F. Fikioris, "Excitation of electromagnetic waves in a gyroelectric cylinder," *IEEE Trans. Antennas Propagat.*, Vol. 33, 90–99, 1985.
22. Chew, W. C., *Waves and Fields in Inhomogeneous Media*, Van Nostrand, New York, 1990.
23. Siqueira, P. R., and K. Sarabandi, "Method of moments evaluation of the two-dimensional quasi-crystalline approximation," *IEEE Trans. Attenas Propagat.*, Vol. 44, 1067–1077, 1996.
24. Tsang, L., J. A. Kong, and R. T. Shin, *Theory of Microwave Remote Sensing*, Wiley, New York, 1985.
25. Pogorzelski, R. J., and E. Lun, "On the expansion of cylindrical vector waves in terms of spherical vector waves," *Radio Sci.*, Vol. 11, 753–761, 1976.
26. Cincotti, G., F. Gori, M. Santarsiero, F. Frezza, F. Furno, and G. Schettini, "Plane wave expansion of cylindrical functions," *Opt. Commun.*, Vol. 95, 192–198, 1983.